실린더로부터 전달되는 혼합대류 열전달의 수치해석(Ⅱ)
Numerical Analysis of Combined Natural and Forced Convection Around Cylinders (Ⅱ)

문 성 홍,* 텐 모 쉬,** 아서 티 존슨***
S. H. Moon,   T. M. Shih,   A. T. Johnson

적 요

실린더로부터 Prandtl 수가 0.7인 주변공기로 전달되는 혼합대류 열전달현상을 Stream-Vorticity 함수로 표시된 지배방정식으로부터 유한차분법으로 분석하였다.

Nusselt 수와 실린더 주변의 온도분포가 조사된 제1편에 이어 Reynolds 수와 Grashof 수가 실린더 주변의 공기속도분포, 경계층 박리지점(Separation point), 실린더 표면에서의 마찰계수 및 실린더 주변에서의 압력 분포에 미치는 영향을 분석하였다.

I. Introduction

Natural convection occurs whenever density gradients exist in a fluid due to the presence of temperature gradients. Therefore, some natural convection always takes place with forced convection heat transfer, but when the externally applied velocity field is dominant, natural convection effects are neglected. Conversely, if the velocity field generated by buoyancy effects is dominant, the forced convection effects, if any, are neglected and the problem is treated as a pure natural convection one. There are also a number of practical situations in which forced convection and natural convection are of the same order of magnitude and neither can be neglected. This is the region of combined natural and forced convection.

Mixed convection around a cylinder can be important in heat tranfer problems from the standpoint of engineering applications as well as numerical analysis. Cylindrically shaped objects occur in many places. Cooling cylindrical cans after sterilization by heat would proceed in the mixed convection mode.

Many vegetables are cylindrical in shape. Examples are radishes and cucumbers. Field conditions often lead to mixed convective heat transfer, because freshly harvested agricultural products are usually much warmer than the fluid used to cool them and fans or pumps are usually inadequate to circulate large amounts of air or water. Accurate predictions of mixed convection heat transfer from cylinders could help to determine the amount of time between harvest and removal from the field to assure adequate

product quality.

Modelling of heat transfer from humans and animals sometimes uses cylindrical elements for similarly shaped anatomical portions such as arms and legs. These models are used to predict thermoregulatory response as well as determine comfort of individuals in various environments. Heat transfer from these surfaces is usually by means of radiation and mixed forced and natural convection.

The cooling of electronic systems may be another application of mixed mode convective heat transfer. To ensure an efficient and viable electronic system, equipment operating temperatures have to be predicted at an early stage of design.

Heat transfer from cylinders has been the subject of numerous analytical and experimental investigations from the standpoint of either pure natural convection (Acrivos[1], Fujii et al[2]., Bejan and Tien[3], Kuehn[4], Ingham[5]) or pure forced convection (Sano[6]), but the problem of combined natural and forced convection from cylinders has received relatively little attention.

Since there is no sharp dividing line between natural and forced convection, it is helpful to define criterion whereby either forced or natural convection effects may be neglected relative to the other. Kreith [7] has made an order of magnitude study of the boundary layer equation for one dimensional flows and concluded that when $GrRe^{-2} > 1$ natural convection effects cannot be ignored in forced flows. Sparrow and Gregg[8] have analyzed the flow over vertical flat plates and have arrived at the conclusion that if an accuracy of 5 per cent is sufficient in computation of overall heat transfer rates, then forced convection heat transfer

results can be used whenever $GrRe^{-2} < 0.255$ for $0.01 < Pr < 10$.

The present research is part II of "Numerical Analysis of Combined Natural and Forced Convection Around Cylinder (I)" presented by Moon[9]. The purpose of this paper is to numerically examine velocity distributions, separation points, drag coefficients and pressures in mixed convection mode around circular cylinders for a wide range of Reynolds numbers and Grashof numbers.

II. Mathematical Formulations

Laminar combined natural and forced convection heat transfer from a horizontal isothermal cylinder is studied by solving the Navier-Stokes equations and energy equation using a finite dfference numerical procedure.

The streamfunction-vorticity equations governing mixed convection steady Boussinesq flow over cylinders can be written in dimensionless and nonconservative form as,

$$-\omega = \frac{\partial^2 \psi}{\partial R^2} + \frac{1}{R} \frac{\partial \psi}{\partial R} + \frac{1}{R^2} \frac{\partial^2 \psi}{\partial \beta^2} \quad \text{......................(1)}$$

$$\frac{\partial^2 \omega}{\partial R^2} + \frac{1}{R} \frac{\partial \omega}{\partial R} + \frac{1}{R^2} \frac{\partial^2 \omega}{\partial \beta^2} = \frac{1}{Pr} (U \frac{\partial \omega}{\partial R} + \frac{V}{R} \frac{\partial \omega}{\partial \beta})$$

$$-PrGr(\sin\beta \frac{\partial \theta}{\partial R} + \frac{\cos\beta}{R} \frac{\partial \theta}{\partial \beta}) \quad \text{....................(2)}$$

$$\frac{\partial^2 \theta}{\partial R^2} + \frac{1}{R} \frac{\partial \theta}{\partial R} + \frac{1}{R^2} \frac{\partial^2 \theta}{\partial \beta^2} = U \frac{\partial \theta}{\partial R} + \frac{V}{R} \frac{\partial \theta}{\partial \beta} \text{ ...(3)}$$

The boundary conditions in stream and vorticity functions become

$$U = V = \psi = 0, \omega = -\frac{\partial^2 \psi}{\partial R^2} , \theta = 1 \quad \text{.................(4)}$$

on the impermeable isothermal cylinder surface and

$$V = \psi = \omega = 0, \frac{\partial U}{\partial \beta} = 0, \frac{\partial \theta}{\partial \beta} = 0 \quad \cdots\cdots\cdots\cdots\cdots (5)$$

on the symmetry lines.

The outer boundary was split into two parts: the area in the plume where the flow leaves the cylinder (namely outflow boundary) and the rest of the boundary where the fluid approaches the cylinder (namely inflow boundary). The inflow boundary conditions at the outer boundary are

$$\psi = -R_\infty Pr Re \sin\beta + \psi_N \quad \cdots\cdots\cdots\cdots\cdots\cdots\cdots (6)$$

$$\omega = -\frac{1}{R_\infty} \frac{\partial \psi}{\partial R} - \frac{1}{R_\infty^2} \frac{\partial^2 \psi}{\partial \beta^2} \quad \cdots\cdots\cdots\cdots\cdots (7)$$

$$\theta = 0 \quad \cdots\cdots\cdots\cdots\cdots\cdots\cdots\cdots\cdots\cdots\cdots\cdots\cdots\cdots (8)$$

The outflow boundary conditions at the outer boundary become

$$\psi = -R_\infty Pr Re \sin\beta + \psi_N \quad \cdots\cdots\cdots\cdots\cdots\cdots (9)$$

$$\omega = -\frac{1}{R_\infty} \frac{\partial \psi}{\partial R} - \frac{1}{R_\infty^2} \frac{\partial^2 \psi}{\partial \beta^2} \quad \cdots\cdots\cdots\cdots\cdots (10)$$

$$\frac{\partial \theta}{\partial R} = 0 \quad \cdots\cdots\cdots\cdots\cdots\cdots\cdots\cdots\cdots\cdots\cdots (11)$$

The numerical procedures for these governing equations and more details were already given in "Numerical Analysis of Combined Natural and Forced Convection Around Cylinder (I)" by Moon[9]. Therefore, in this paper, they will be omitted.

III. Results and Discussion

The two independent parameters for this investigation are the Reynolds and Grashof numbers. The effects of these parameters on velocity distributions, separation points, drag coefficients and pressure distributions about circular cylinders were presented. The Prandtl number was maintained at a value of 0.7, which is the value for air.
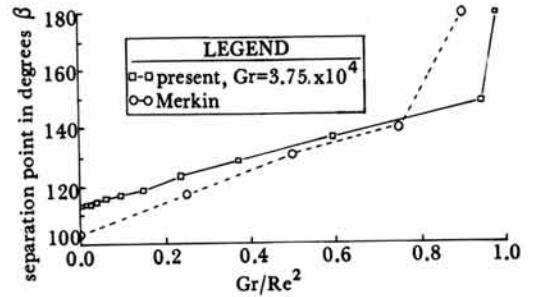

Fig. 1. Comparison of numerical separation point versus mixed convection parameter for cylinders

Comparison of the separation points in the present study and that by Merkin (1977)[10] is shown in Figure 1. Both studies predict that the separation point is delayed as Gr/Re^2 increases. This trend suggests that the buoyancy force tends to reduce the adverse pressure and consequently accelerate the flow. Despite the qualitative agreement, significant quantitative difference is observed. A possible explanation for this disagreement is that, in Merkin's data, the flow was assumed to be of the boundary layer type. Clearly the flow near the stagnation region or at small Re and Gr values (when diffusion in both angular and radial directions are of equal strength) cannot be adequately governed by the boundary layer equations.

Figure 2 separation points in angles versus Reynolds number for the cylinder are plotted at various Grashof numbers. The results show that, as the Reynolds
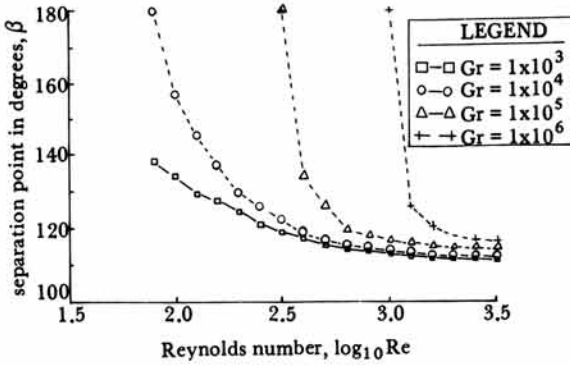
Fig. 2. Variation of the separation point for cylinders with Reynolds numbers at various Grashof numbers.

number increases, the separation point occurs at lower angles and then remains almost stationary above certain Reynolds numbers. These constant locations are reached earlier at lower Reynolds number as Grashof numbers decrease. This means that buoyancy force retards earlier separation. For purely forced flow about cylinders analyzed with steady-state boundary layer equations, Schlichting (1979)[11] said that the point of separation occurred at $\beta=108.8°$ for cylinder.

Drag coefficient may be one of primary interest to study. Drag coefficient C_f is usually defined as (Ozisik, 1977)[12]

$$C_f = \frac{2\tau_w}{\rho u_\infty^2} \quad \text{.........................(12)}$$

where

$$\tau_w = \mu \left(\frac{\partial v}{\partial r}\right)_{r=r_o} \quad \text{...........................(13)}$$

τ_w = shear stress
C_f = drag coefficient
ρ = fluid density
U_∞ = undisturbed oncoming free stream velocity
μ = fluid dynamic viscosity
v = angular velocity

r = radial coordinate
r_o = cylinder radius

With dimensionless variables,

$$Pr = \frac{\nu}{\alpha} \quad \text{.................................(14)}$$

$$Re = \frac{Du_\infty}{\nu} \quad \text{..............................(15)}$$

$$V = v\frac{D}{\alpha} \quad \text{...................................(16)}$$

$$R = \frac{r}{D} \quad \text{.......................................(17)}$$

where

Pr = Prandtl number
ν = fluid kinematic viscosity
α = fluid thermal diffusivity
Re = Reynolds number
V = dimensionless angular velocity

Equation 12 can be transformed into

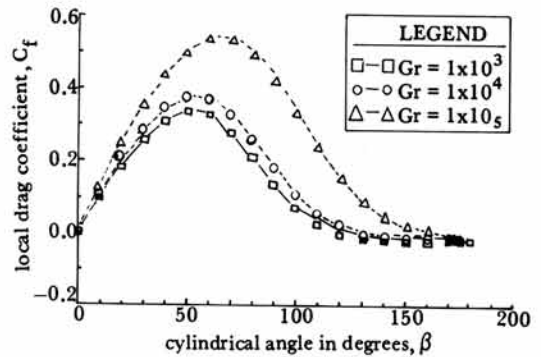$$C_f = \frac{2(\partial V/\partial R)_{R=0.5}}{PrRe^2} \quad \text{......................(18)}$$

Fig. 3. Variation of local drag coefficient with cylindrical angle at various Grashof numbers for Re=199.53

Figures 3 and 4 illustrate the angular distributions of the drag coefficient at various parametric values of Gr or Re for the cylinder. It can be seen from the figures that the local wall shear stress, τ_w, increases with increasing buoyancy force with a resulting delay in the flow separation. This is because
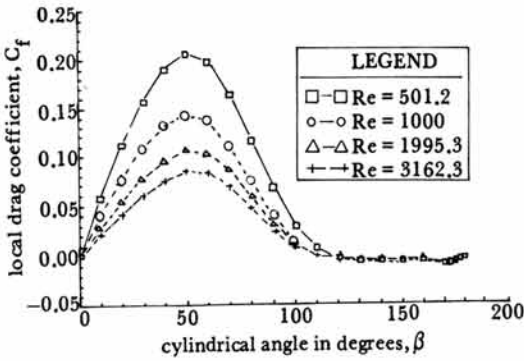
Fig. 4. Variation of local drag coefficient with cylindrical angle at various Reynolds num-
bers for Gr=3.75×10⁴

the buoyancy force in the flow domain assists the forced flow in acting against the adverse pressure gradient. As Reynolds number increases, the drag coefficient decreases at fixed Grashof number. In fact, as Reynolds number increases, wall shear stress should increase but the undisturbed free stream velocity, u_∞, may also increase faster. Therefore, according to the drag coefficient definition (equation 18) the drag coefficient decreases as Reynolds number increases. The drag coefficient is almost zero at the place where separation occurs. The average drag coefficients versus Reynolds number at various Grashof numbers are plotted in
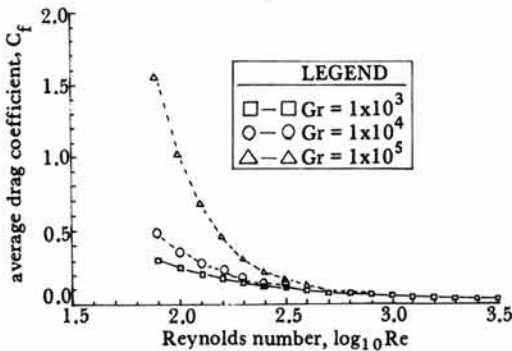

Fig. 5. Variation of average drag coefficient with Reynolds number at various Grashof num-
bers for cylinders

Figure 5 for the cylinder.

The average drag coefficient increases as Grashof numbers increase since the buoyancy flow aids the forced flow stream significantly. When the Reynolds numbers are more than 500, the average drag coefficient has almost the same values for any given Grashof numbers because the increasing rate of wall shear stress gained by buoyancy force effects is relatively small in comparison with the increasing rate of undisturbed free stream velocity, u_∞, for the increasing Reynolds number. At lower Grashof numbers the average drag coefficient decreases monotonically as Reynolds number increases. This tendency is consistent with that of the drag coefficient for purely forced flow presented by Schlichting (1979)[11]
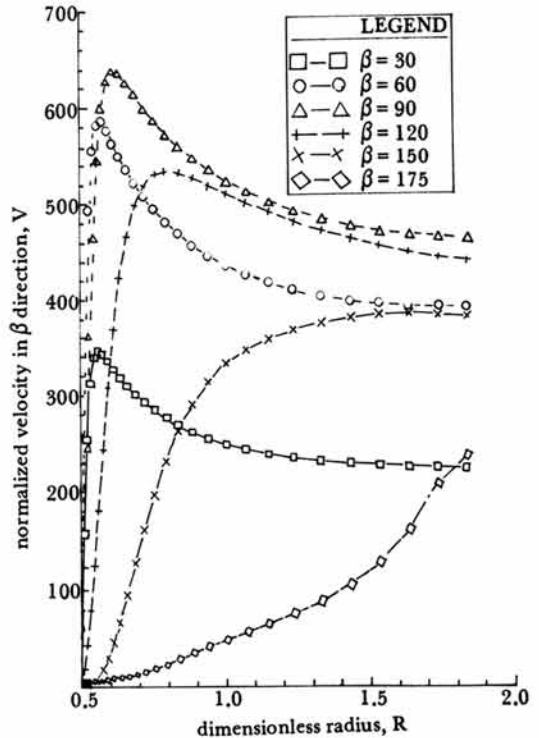
Angular velocity distributions as func-

Fig. 6. Angular velocity distribution at various cylindrical angles for Gr=3×10⁵ and Re=500

tions of dimensionless radius R at several angular locations are given in Figure 6 for the cylinder.

The velocities near the wall have almost the same values for angles between 0 to 90 degrees. The angular velocities for angles between 0 to 90 degrees increase rapidly until reaching about 0.6 of the dimensionless radius and then those velocities decrease gradually as radius increases. The angular velocities for angles larger then $150°$ always increase as the radius increases. The angular velocity drops to zero at $180°$. In the natural convection analysis, Kuehn (1980)[4] mentioned that in the plume, $\beta \geq 175°$, the angular velocity was a function only of the horizontal distance from the plume center line and is independent of distance above the cylinder. However, in mixed convection, the velocity profiles are quite different from those of natural convection since the separation point occurs because of the effects of forced flow.

The radial velocity distributions versus dimensionless cylindrical radius R at $G= 3 \times 10^5$ and Re=500 are given in Figure 7. For a given angle, radial velocities are fairly uniform around the outer portions of the computational domain except for the case of $180°$. This is shown by the curves from $\beta=0°$ to $\beta=150°$. As expected, the radial velocity at $\beta=90°$ is fairly close to zero except in the region near the wall which is affected by the buoyancy force. If the forced convection flow predominates, even near the wall, the radial velocity at $\beta=90°$ would be zero. At the $180°$ angle, the radial velocity increases rapidly as radial distance becomes larger. At the outer boundary at $\beta=180°$, the velocity becomes largest with almost double the
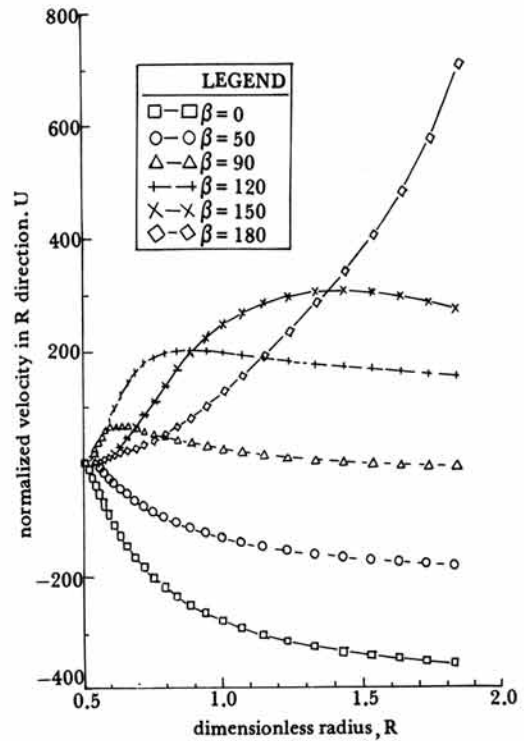

Fig. 7. Radial velocity distribution at various cylindrical angles for Gr=3×10^5 and Re=500

values of undisturbed free stream velocity, u_∞, in absolute values due to the aiding flow of buoyancy force.

Figure 8 shows the pressure distribution along the cylindrical surface versus cylindrical angle β for various values of Froude number at $Gr=10^4$ and Re=100. Intuitively, it is
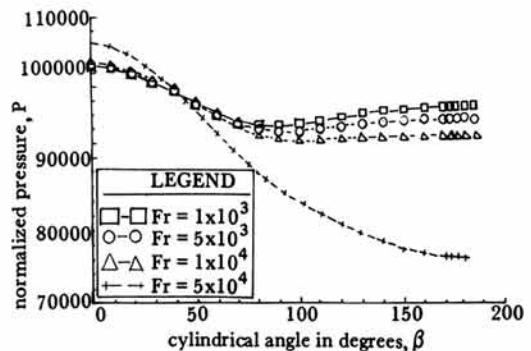

Fig. 8. Pressure distribution versus cylindrical angle at Cr=10 and Re=100 for various Froude numbers.

expected that pressure, P, will assume large values at the stagnation point ($\beta=0°$) and will decrease as β increases. Then, as β increases, the pressure will start increasing since it is known (Schlichting, 1979)[11] that the fluid particles are accelerated on the upstream half and decelerated on the downstream half of the cylinders. This intuition is confirmed by the trend exhibited in the figure for small Froude numbers. For large Froude numbers, however, the pressure decreases monotonically with β. An explanation of this trend is needed and may be attempted as follows. On the cylindrical surface, the V-momentum equation can be reduced to

$$\left(\frac{\partial P}{\partial \beta}\right)_{R=.5} = \frac{1}{2}\sin\beta Pr^2(Gr\text{-}Fr) + Pr\frac{\partial}{\partial R}\left(R\frac{\partial v}{\partial R}\right)_{R=0.5}$$

....(19)

where

P = dimensionless pressure

Fr = Froude number, gD^3/ν^2

g = gravitational acceleration

D = cylinder diameter

ν = kinematic viscosity

in dimensionless form. Interestingly, the value of $\partial P/\partial \beta$ is determined by the sum of two terms in the right hand side of equation 19. The first term represents the buoyancy term and is negative if Froude number, Fr, is larger than Grashof number, Gr. The second term represents the radial gradient of the shear stress and is generally negative since, at a fixed β, the shear stress on the wall assumes a large value. In the vicinity of the symmetry line where β is small, the first term involving $\sin\beta$ is small and the value of $\partial P/\partial \beta$ is likely to be negative. When β increases, the magnitude of the buoyancy term increases, and $\partial P/\partial g$ can become positive

thereafter. If the Froude number is large, however, both terms are negative even at large β. Consequently, P decreases monotonically as β increases.
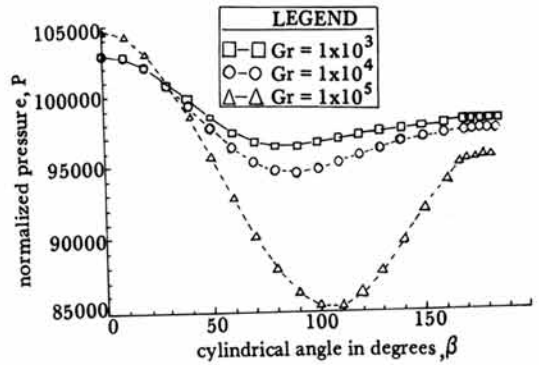

Fig. 9. Pressure distribution versus cylindrical angle at Fr/Gr=0.1 and Re=100 for various Grashof numbers

Figure 9 show the effects of Grashof number on the pressure distribution around cylindrical surface for various values of Grashof number at Re=100 and Fr=0.1xGr. At cylindrical angles over about 30 degrees pressure decreases as the Grashof number increases, since the fluid particles are accelerated by the buoyancy force. The effects of Reynolds number on the pressure and the forced convection effects on the natural convection flow can be examined in Figure
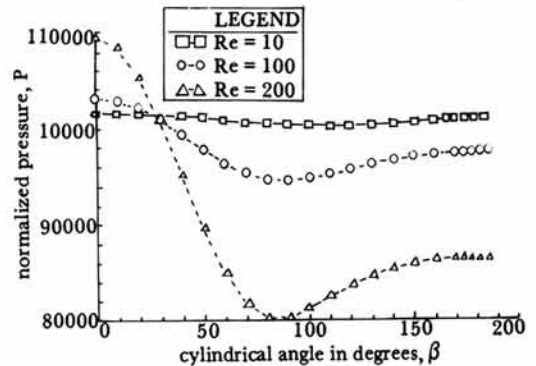

Fig. 10. Pressure distribution versus cylindrical angle at Fr=10^3 and Gr=10^4 for various Reynolds numbers

10 for the cylinder.

For various Reynolds numbers at $Gr=10^4$ and $Fr=10^3$. For pure natural convection or low Reynolds number flows, the pressures on the surfaces appear fairly uniform. As the ambient fluid is driven faster, pressure minima appear around $\beta=90°$. This significant difference between natural convection and mixed convection deserves attention.

IV. Conclusions

1. As Reynolds number increases, the separation point occurs at lower angles and remains almost constant at high Reynolds numbers.

2. The local wall shear stress increases with increasing buoyancy force with a resulting delay in the flow separation.

3. Angular velocities for angles between 0 to 90 degrees increase rapidly until reaching about 0.6 of the dimensionless radius, and those velocities decrease gradually as radius, R, increases.

4. From the V-momentum equation on the cylindrical surface,

$$\left(\frac{\partial P}{\partial \beta}\right)_{R=.5} = \frac{1}{2}\sin\beta P^2 r (Gr-Fr)+Pr\frac{\partial}{\partial R}\left(R\frac{\partial V}{\partial R}\right)_{R=0.5}$$

the trend of radial pressure gradient is examined. The value of $(\partial P/\partial \beta)_{R=0.5}$ is determined by the sum of two terms in the right hand side of above equation. The first term represents the buoyancy term and is negative if Froude number, Fr, is larger than Grashof number, Gr. The second term represents the radial gradient of the shear stress and is generally negative.

References

1. Acrivos, A.A. 1960. A Theoretical Analysis of Laminar Natural Convection Heat Transfer to Non-Newtonian Fluids. AICHE Journal, 6:584-590.

2. Fujii, T., M. Fujii and T. Matsunaga. 1979. A Numerical Analysis of Laminar Free Convection around an.

3. Bejan, A. and C.L. Tien. 1979. Natural Convection in Horizontal Space Bounded by Two Concentric Cylinders with Different End Temperatures. Int. J. Heat. Mass transfer, Vol. 22:919-927.

4. Kuehn, T.H. and R.J. Goldstein. 1980. Numerical Solution to the Navier-Stokes Equations for Laminar Natural Convection about a Horizontal Isothermal Circular Cylinder. Int. J. Heat Mass Transfer, vol. 23:971-979.

5. Ingham, D.B. 1981. Heat Transfer by Natural Convection between Spheres and Cylinders Numerical Heat Transfer, Vol. 4:53-67.

6. Sano, T. 1978. Shrot-Time Solution for Unsteady Forced Convection Heat Transfer from an Impulsively Started Circular Cylinder. Int. J. Heat Mass Transfer, vol. 21:1505-1516.

7. Kreith, F. 1965. Principles of Heat Transfer, Second Edition. International Textbook Co., Scranton, Pa.

8. Sparrow, E.M. and J.L. Gregg. 1959. Buoyancy Effects in Forced Convection Flow and Heat Transfer. J. Appl. Mech., 81:133-134.

9. Moon, S.H. 1986. Numerical Analysis of Combined Natural and Forced Convection Around Cylinders (I). — Nusselt Numbers and Mixed Convection Para-

meters—. The Journal of the Korean Society for Agricultural Machinery, vol. 11, No. 1.

10. Merkin, J.H. 1977. Mixed Convection from a Horizontal Circular Cylinder. Int. J. Heat Mass Transfer, vol. 20: 73-77.

11. Schliching, H. 1979. Boundary Layer Theory. McGraw-Hill Co., Incorporated, New York, New York.

12. Ozisik, M.N. 1977. Basic Heat Transfer. McGraw-Hill Co., Incorporated, New York, New York.

▶ 原 稿 募 集 ◀

韓國農業機械學會誌에 揭載할 原稿를 아래와 같이 募集하오니 會員 여러분의 많은 投稿 바랍니다.

아　　래

- 原稿의 種類 : 投稿規定 第2項 參照
- 投 稿 要 領 : 投稿規定 參照(61~62 參照)
- 原 稿 接 受 : 隨時接受(단 3月號의 원고접수마감은 2月 15日임)
- 送 付 處 : 京畿道 水原市 西屯洞 103番地
　　　　서울大學校 農科大學 農工學科內 韓國農業機械學會